Structure and Equilibrium of Four Molecular Clouds from the BU–FCRAO Milky Way Galactic Ring Survey

R. Simon, J.M. Jackson, T.M. Bania, D.P. Clemens, and M.H. Heyer[1]

Institute for Astrophysical Research, Boston University

[1]Five College Radio Astronomy Observatory, University of Massachusetts, Amherst

Abstract

We present a study of the structure of four molecular clouds from the BU-FCRAO Milky Way Galactic Ring Survey (GRS), a high resolution study of ^{13}CO J=1→0 in the first Galactic quadrant using the FCRAO 14 m telescope. The clouds span a large range of star formation activity, from W49, the most luminous star forming region in the Milky Way, to G045.46+0.05, which has no obvious star formation activity. We use a three-dimensional gaussian decomposition to identify clumps and study their properties, including sizes, masses, and line widths.

Every cloud has the same clump mass spectrum independent of star formation activity. Relations of clump size with mass and density differ from the conventional Larson relations and the line width shows only a weak dependence with clump size.

While the clouds as a whole are in gravitational virial equilibrium, most clumps are not gravitationally bound. Star forming clouds have a much higher fraction of gravitationally bound clumps than non star forming clouds. The unbound clumps are possibly confined by the weight of the self-gravitating complex. The pressures needed to bind these clumps are largest for the star forming clouds.

For more and future information visit the GRS web page:
http://carp.bu.edu/grs/

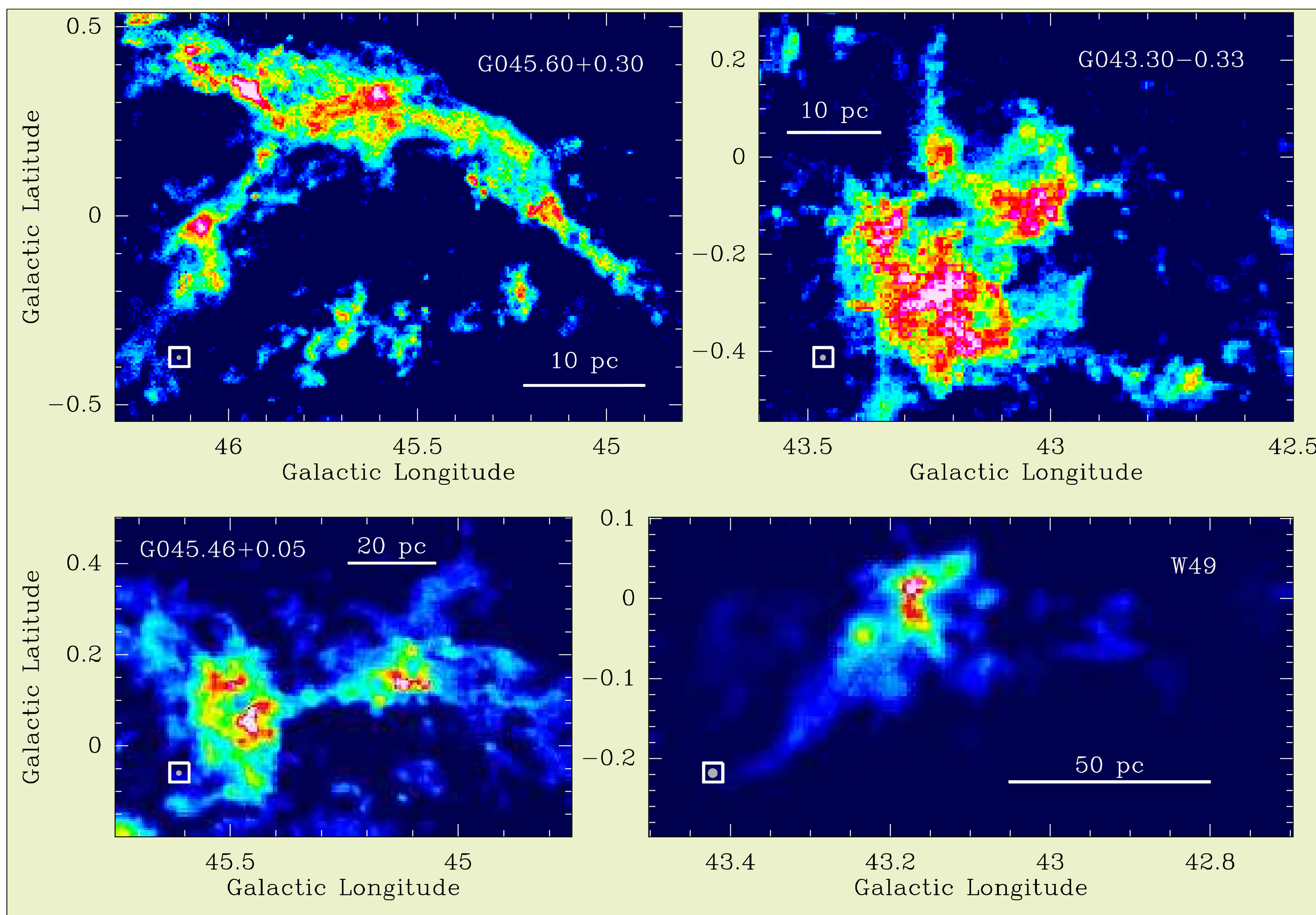

Fig. 1: *Color scale representation of zeroth moment maps of the GRS ^{13}CO intensity integrated over the specified velocity range relevant for emission from the individual cloud complexes. The top panels show two clouds without star formation and the bottom panels display the star forming clouds. The plot ranges are:* **Top:** *^{13}CO integrated intensity from 1.3 to 7.5 K km s^{-1} (left panel) and 2.6 to 68.7 K km s^{-1} (right panel).* **Bottom:** *^{13}CO integrated intensity from 1.1 to 10.3 K km s^{-1} (left panel) and 3.2 to 158.5 K km s^{-1} (right panel). The beam size is indicated in the lower left corner of each panel. The linear size scales were determined assuming the distances given in Table 1.*

Introduction

When observed at increasingly higher linear resolution, molecular clouds typically reveal a rich clumpy structure, often self-similar or filamentary. The observed properties of the clouds and the clump ensembles yield important information on the effects of turbulence and self-gravity, which are believed to generate cloud substructure, and the process of star formation itself. Since the GRS covers large areas of the sky on a Nyquist-sampled grid, with high angular and spectral resolution, it constitutes a unique data base for the investigation of molecular cloud structure within the first Galactic quadrant.

To evaluate the internal structure of Giant Molecular Clouds in the Inner Galaxy, we have analyzed four subfields within the ongoing BU-FCRAO Galactic Ring Survey. The selected clouds (Fig. 1) cover a wide range of star formation activity. Coordinates and distances are summarized in Table 1.

Table 1: Molecular clouds selected for this study.

Cloud[a]	Longitude	Latitude	v_{LSR} (km s^{-1})	Distance (kpc)
G45.6+0.3	45.60	+0.30	25.0	1.8[b]
G43.3−0.3	43.30	−0.33	40.0	3.0[b]
G45.5+0.1	45.46	+0.05	60.0	6.5[b]
W49	43.17	+0.00	11.2	11.4[c]

[a]Position of a prominent ^{13}CO emission peak.
[b]Distances determined kinematically (see Jackson et al., 25.03).
[c]Distance from Gwinn, Moran, & Reid (1992, ApJ, 393, 149).

We model the three-dimensional (two spatial and one velocity) data as Gaussian-shaped clumps using the algorithm developed by Stutzki & Güsten (1990, ApJ, 356, 513).

Clump-Mass Spectra

The clump masses are determined using the fitted ^{13}CO clump brightness temperatures and line widths in an optically thin LTE approximation at an excitation temperature of 10 K. We applied conversion factors of R(^{12}CO/^{13}CO) = 45 adopted from Langer & Penzias (1990, ApJ, 357, L477) and X(^{12}CO/H_2) = 8×10^{-5} (Blake et al. 1987, ApJ, 315, 621), as well as a correction to the hydrogen mass of a factor of 1.36 to account for helium and other heavy elements (Allen 1973, Astrophysical Quantities). The clump mass in Solar masses is given by

$$M_{LTE} = 2.67 \times 10^{-10}\, T_{mb} \Delta v\, \theta_x \theta_y\, D^2$$

where θ_x and θ_y are the sizes of the principal half-axes of the clump in arcseconds and D is the distance to the cloud in pc. The resulting clump-mass spectra $dN/dM \propto M^{-\alpha M}$ are shown in Fig. 2.

We do not find any significant differences in the clump-mass spectra of the star forming and non star forming clouds.

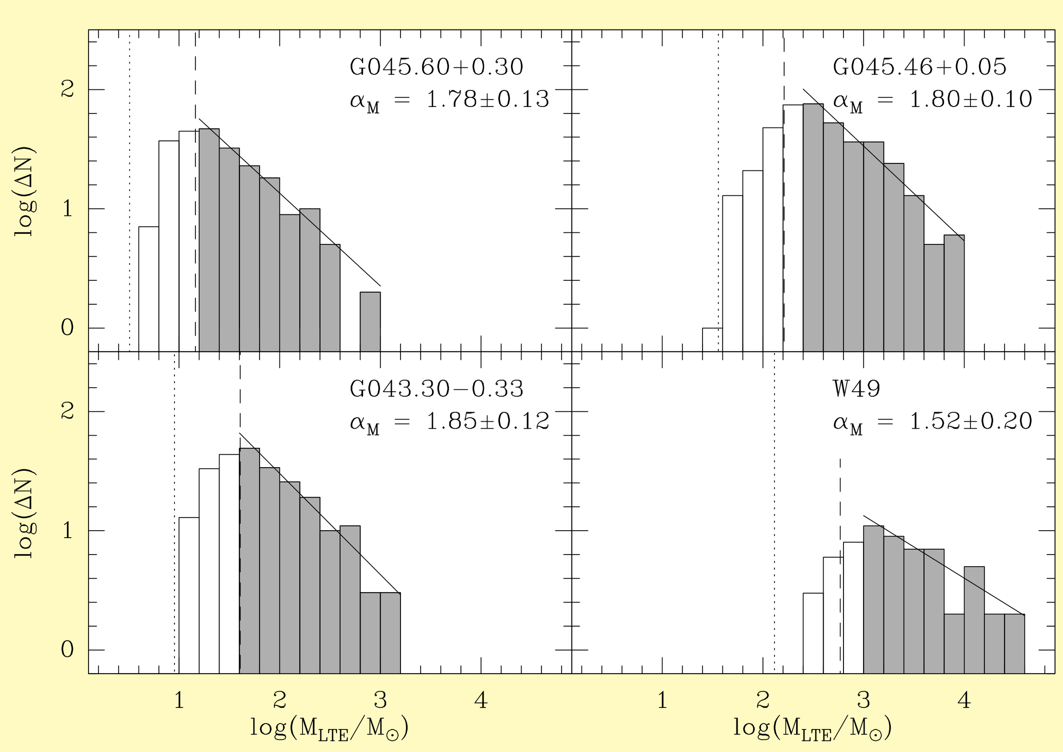

Fig. 2: *Clump-mass spectra of the four GRS clouds. Star forming clouds are on the right. Only masses well above the completeness limit (dashed line, bins indicated by the filled histogram columns), were used in a fit to derive α_M. A dotted vertical line is drawn at the value of the minimum clump mass we allowed the algorithm to find. The errors have been evaluated by taking into account the $\Delta N^{1/2}$ statistical error for each mass bin.*

Scaling Relations

Once the clumps are identified, general trends in their properties (e.g. mass, size, density, and line width) are used to characterize cloud structure. Although applying different methods, many studies arrive at consistent results for scaling relations with the sizes of structures as first pointed out by Larson (1981, MNRAS, 194, 809).
The corresponding relations for the four GRS clouds are plotted in Fig. 3 and the results (including the dispersion) are compared to the relations for virial equilibrium in Table 2.

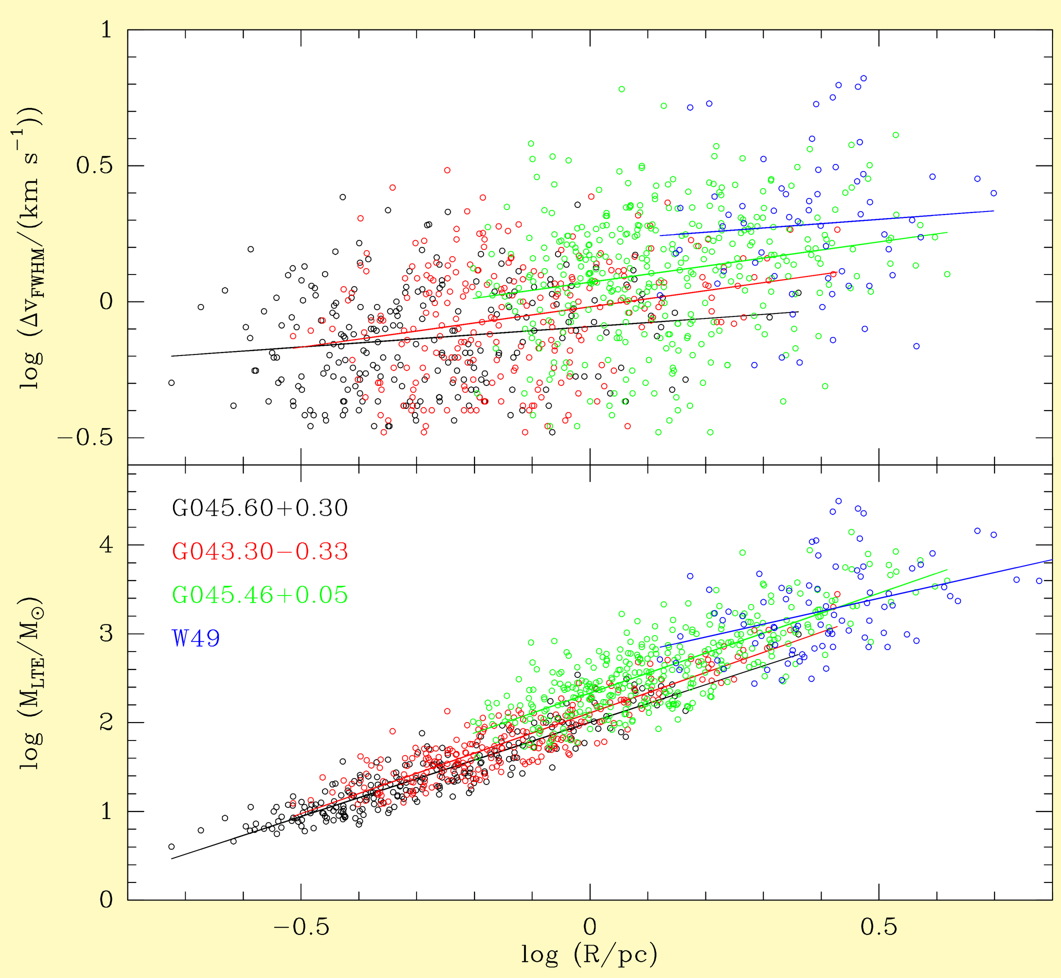

Fig. 3: *Relation of clump size with line width and mass of the clumps for the GRS clouds. Clumps in star forming clouds are represented by green and blue symbols. Straight lines represent least squares fits to the slopes. The power law indices (including the dispersion) are included in Table 2. Note that, due to redundancy, results for the size-density relation are not shown in the plot. The different ranges in size are partly due to the different distances to the clouds.*

Table 2: Summary of power law relations for the clumps.

Cloud	Density	Size-Line width	Mass	Mass spectrum
G45.6+0.3	0.86 (0.33)	0.15 (0.33)	2.21 (0.33)	1.78 (0.13)
G43.3−0.3	0.73 (0.35)	0.30 (0.35)	2.27 (0.35)	1.85 (0.12)
G45.5+0.1	0.75 (0.32)	0.29 (0.32)	2.25 (0.32)	1.84 (0.10)
W49	0.84 (1.01)	0.16 (1.01)	2.15 (1.01)	1.56 (0.20)
Weighted Mean	0.78(0.19)	0.24(0.19)	2.24(0.19)	1.80(0.10)
Virial Equilibrium	1.0	0.5	2.0	

Our relations of clump size with density, line width, and mass systematically differ from the conventional scaling relations for virial equilibrium. The size-line width relation is flatter and the size mass relation steeper, resulting in a weak dependence of the surface density with mass.

Equilibrium

The equilibrium state of the clumps is deduced from the comparison of virial and LTE mass of the clumps shown in Fig. 4. While the cloud complexes as a whole are gravitationally bound, most of the clumps are unbound. This explains the above shown deviation from the standard Larson relations which are only valid for objects in virial equilibrium. It turns out that the pressures needed to confine the unbound objects are possibly provided by the overlying weight of the bound complex and are largest for the star forming clouds. Under this assumption, most of the overpressured clumps will not be transient. The magnitude of the binding pressures points towards a higher external pressure in the Inner Galaxy compared to the Outer Galaxy.

The histograms shown in Fig. 5 are used to evaluate the fraction of gravitationally bound clumps in the clouds.

The Galactic Ring Survey acknowledges support by the NSF via grant AST–9800334.

National Science Foundation
Celebrating 50 Years

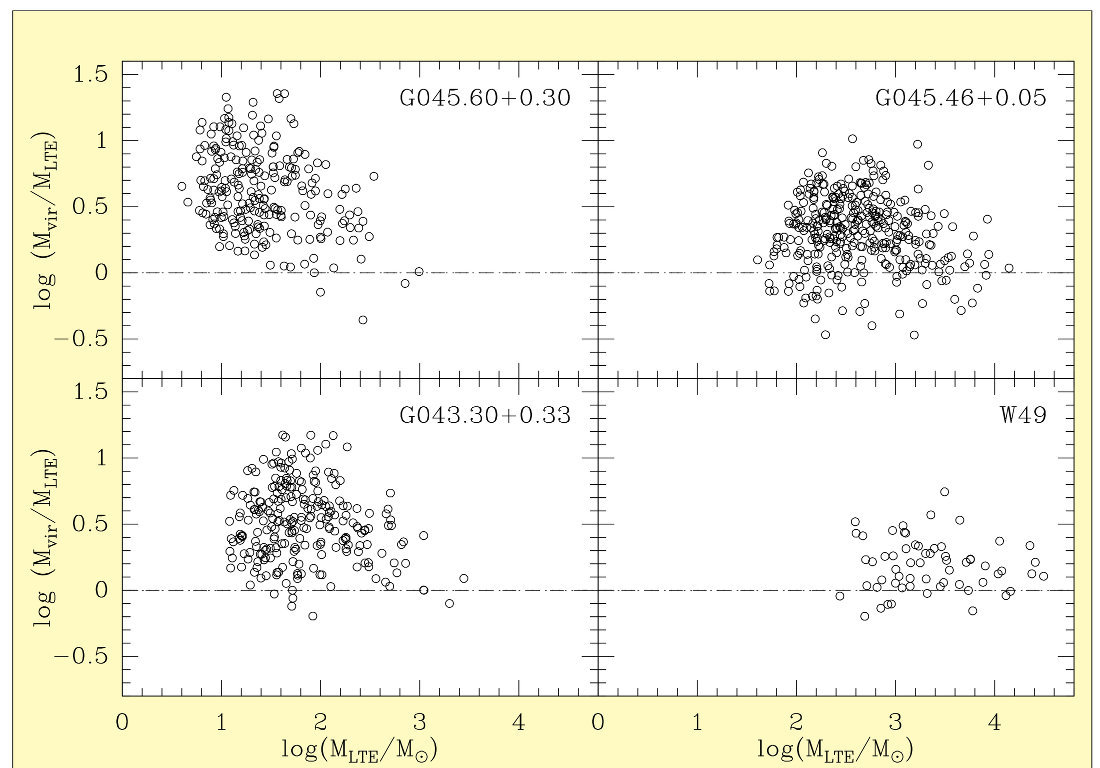

Fig. 4: *The ratio of virial to LTE mass for the clumps in the GRS clouds. Star forming clouds are on the right. The dotted line represents gravitational virial equilibrium: Clumps below this line are gravitationally bound.*

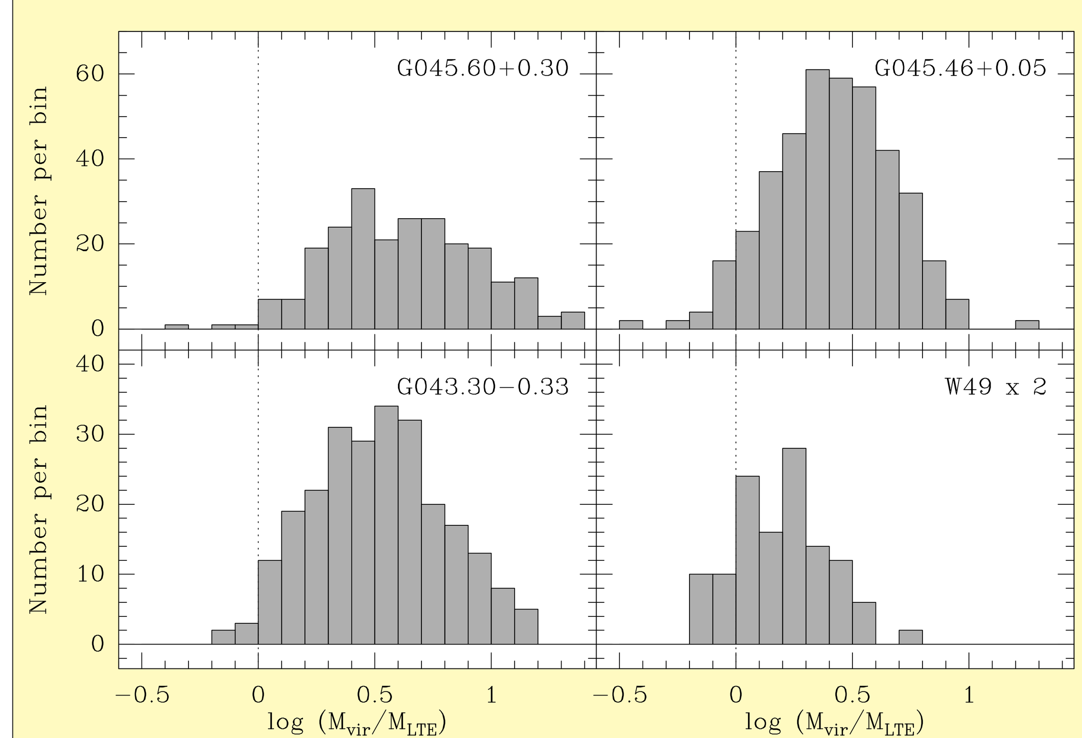

Fig. 5: *Histograms of the ratio of virial to LTE mass for the clumps. Star forming clouds are on the right. The dotted line corresponds to $M_{vir} = M_{LTE}$: Clumps to the left of this line are gravitationally bound.*

In order to test whether our results are influenced by spatial resolution, we smoothed the nearest cloud G45.6+0.3 to a five times larger distance. Results of our standard clump decomposition applied to this data set (see Fig. 6 below) reveal the same qualitative properties of clumps at high and low angular resolution.

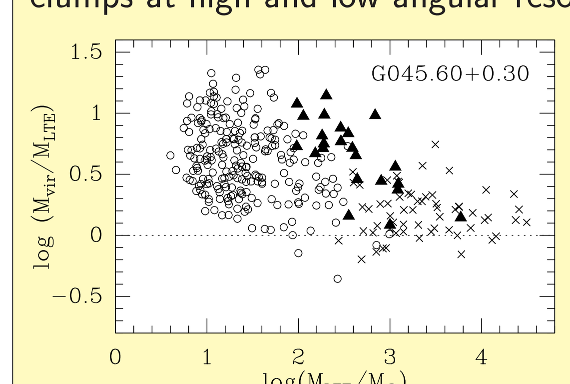

Fig. 6: *Ratio of virial to LTE mass for the non star forming cloud G45.6+0.3 with the full resolution (circles) and smoothed to a five times larger distance (triangles).*

We conclude that the star forming clouds have a higher fraction of gravitationally bound clumps than the non star forming clouds.

Conclusions

- We find no difference in the clump-mass spectra of the GRS clouds over a wide range of clump masses and star formation activity.
- The properties of the clumps inside the clouds show systematic deviations from the standard relations for virial equilibrium.
- The molecular cloud complexes are gravitationally bound; most of the clumps inside the clouds are gravitationally unbound and confined by the weight of the complex.
- The star forming clouds have a higher fraction of gravitationally bound clumps than the non star forming regions.